The Proton Affinity of the Superbase 1,8-Bis(tetramethylguanidino)naphthalene (TMGN) and Some Related Compounds: A Theoretical Study

Borislav Kovačević and Zvonimir B. Maksić*[a]

Dedicated to Professor Rolf Gleiter on the occasion of his 65th birthday

Abstract: The spatial and electronic structure of the very strong neutral organic bases bis(tetramethylguanidino)naphthalene (**TMGN**), 4,5-bis(tetramethylguanidino)fluorene (**TMGF**) and some related compounds are explored by ab initio computational methods. Their affinity towards the proton is scrutinized both in the gas phase and in solution in acetonitrile. The protonation at the most basic center (the imine nitrogen) yields asymmetric and relatively strong intramolecular hydrogen bonds (IHB). It is found that the angular strain effect and steric repulsion practically vanish in **TMGN** which implies that its high absolute proton affinity (APA) has its origin in the inherent basicity of the guanidine fragment and a relatively strong IHB in [**TMGN**]H^+. The nonbonded repulsions in **TMGF** are higher than in **TMGN**, which in conjunction with a slightly stronger IHB in the corresponding conjugate acid makes it more basic: APA(**TMGF**) > APA(**TMGN**). An interesting new phenomenon is observed in both TMGN and TMGF: the proton triggers the resonance stabilization not only in the directly bonded guanidine moiety, but also in the other guanidine fragment which is more distant from the proton, albeit in a less pronounced manner. The latter feature is termed a *partial protonation*. This supports the hydrogen bonding and contributes to the IHB stabilization. Convincing evidence is presented that the solvent effect in acetonitrile is determined by two antagonistic factors: 1) the intrinsic (gas phase) proton affinity and 2) the size effect which is given by the ratio between the positive charge in molecular cation (conjugate acid) and the magnitude of the molecular surface. The resulting pK_a values are given by an interplay of these factors.

Keywords: basicity · proton affinity · protonation · proton sponges

Introduction

Preparation and characterization of neutral organic bases has been a subject of considerable interest for a large number of researchers for several decades.[1, 2] This is not surprising, as strong neutral bases have some distinct advantages over their ionic counterparts. They require milder reaction conditions and possess an increased solubility at the same time.[3] Consequently, neutral organic (super)bases have found a wide range of applications in syntheses as auxiliary base mediators.[4] The first molecule to be prepared of this class of compounds was the paradigm, 1,8-bis(dimethylamino)naphthalene (**DMAN**), which has been subsequently followed by a large number of diamine derivatives.[5]

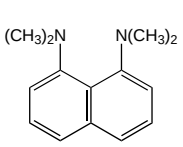

DMAN

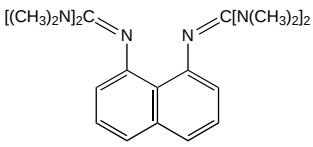

TMGN

Lately, considerable attention has been focused on imines,[6] polyfunctional formamidines,[7] vinamidines[8] and phosphazenes,[9] in which the most susceptible position for the proton attack was provided by the imine nitrogen atom. Concomitant with extensive experimental investigations, there is an increasing number of the theoretical studies of proton affinities of organic molecules,[10–17] with an emphasis on the design of new neutral organic superbases.[18–24] These computational investigations have shown that a high basicity can be expected if the resulting conjugate acids are stabilized by the aromatization of a molecular backbone, which may consist of sequential quinoimine[20] and/or cyclopropenimine[21] subu-

[a] Prof. Dr. Z. B. Maksić, Dr. B. Kovačević
Quantum Chemistry Group, Rudjer Bošković Institute
Bijenička c. 54, 10000 Zagreb-HR (Croatia)
and Faculty of Science and Mathematics University of Zagreb
Marulićev trg 19, 10000 Zagreb-HR (Croatia)
E-mail: zmaksic@spider.irb.hr

0947-6539/02/0807-1694 $ 20.00+.50/0

nits. Another interesting structural and electronic motif is given by guanidine fragments, which undergo a very strong cationic resonance stabilization that is triggered by protonation.[23] Juxtaposition of guanidine and other suitable subunits such as cyclopropenimines also yields powerful superbases.[24] Apparently, combinations of different motifs offer a large variety of strong bases, which exhibit a wide range of proton affinities.

The present work was motivated by the synthesis of the eponymous compound 1,8-bis(tetramethylguanidino)naphthalene (**TMGN**) by Raab et al.[25] This intriguing system has led to simultaneous experimental[25] and theoretical examinations of its structure, properties and proton attracting ability in the gas phase and in acetonitrile. We describe the theoretical investigations in this paper. In addition, we consider some related molecules, which place **TMGN** in a proper perspective and help to elucidate its superbasicity.

Methodology

Absolute proton affinities (APA) in the gas phase are computed in the following standard manner:

$$\mathrm{APA}(\mathrm{B}_\alpha) = (\Delta E_{\mathrm{el}})_\alpha + (\Delta \mathrm{ZPVE})_\alpha \quad (1)$$

$$(\Delta E_{\mathrm{el}})_\alpha = E(\mathrm{B}) - E(\mathrm{B}_\alpha\mathrm{H})^+ \quad (2)$$

$$(\Delta \mathrm{ZPVE})_\alpha = \mathrm{ZPVE}(\mathrm{B}) - \mathrm{ZPVE}(\mathrm{B}_\alpha\mathrm{H})^+ \quad (3)$$

B and BH^+ denote the base in question and its conjugate acid, respectively, whilst α stands for the site of proton attack. Equations (2) and (3) give the electronic and zero point vibrational energy contributions to the proton affinity, respectively. The search of the Born–Oppenheimer energy hypersurfaces has been performed with the efficient Hartree–Fock level by the use of the 6-31G* basis set. One of the results of the present study is that the HF/6-31G* geometries are in accordance with the experimental data.

The minima on the hypersurface that correspond to equilibrium geometric structures are verified by vibrational analyses at the same level. The calculated vibrational frequencies are used in deriving the ZPV energies by the application of a common scale factor, 0.89, as customary. The final single point calculations take into account the fact that a proper description of the nitrogen lone pairs requires the use of the flexible 6-311 + G** basis set, and that reliable estimates of the proton affinity require an explicit account of the electron correlation energy at least to the level of Møller–Plesset (MP) perturbation theory of the second order. This gives rise to the MP2(fc)/6-311 + G**//HF/6-31G* + ZPVE(HF/6-31G*) model,[17] which will be referred to henceforth as MP2. The calculations of the solvent effect in acetonitrile will be described later (see below). All computations are carried out by using GAUSSIAN 94 and GAMESS programs.[26, 27]

Abstract in Croatian: *Primjenom ab initio metoda istražena je prostorna i elektronska struktura vrlo jakih neutralnih organskih baza **TMGN** i **TMGF** zajedno s nekim srodnim spojevima. Odredjeni su njihovi protonski afiniteti kako u plinskoj fazi tako i u acetonitrilu. Najveću sklonost prema protonu ima iminski atom dušika gvanidinskog fragmenta. Protoniranjem se stvara asimetrična vodikova veza (IHB) kako kod **TMGN** tako i kod **TMGF**. Pokazuje se da su kutna napetost i steričko odbijanje praktički jednaki nuli kod prve molekule. Iz toga proizlazi da je visoki apsolutni protonski afinitet (APA) **TMGN**-a posljedica imanentne bazičnosti gvanidinskog fragmenta kao i relativno jake vodikove veze. Kod **TMGF**-a nevezne interakcije i nešto jača IHB u konjugiranoj kiselini vode na izraženiju lužnatost ovog spoja: APA(**TMGF**) > APA(**TMGN**). Vrlo interesantna pojava opažena je kod obje ove molekule: proton odapinje rezonantnu stabilizaciju ne samo u onom gvanidinskom fragmentu, koji je direktno vezan na proton, već i u njegovom vis-à-vis partneru. Može se kazati da je ovaj potonji parcijalno protoniran. Stabilizacijske promjene u njemu su manje ali značajne, što pridonosi jačini IHB. Ustanovljeno je da na bazičnost neutralnih organskih baza u acetonitrilu utječu dva faktora: 1) inherentni ili prirodjeni protonski afinitet baze i 2) veličina molekularne površine konjugirane kiseline. Rezultirajuće pK_a vrijednosti rezultanta su ova dva utjecaja.*

Results and Discussion

Spatial structures: Naphthalene **1**, **TMGN 2**, its protonated and diprotonated forms **2p** and **2dp**, are shown in Figure 1, together with 1-tetramethylguanidinonaphthalene, **3**, and its most stable conjugate acid, **3p**. Some relevant structural parameters obtained by the HF/6-31G* model are presented in Table 1.

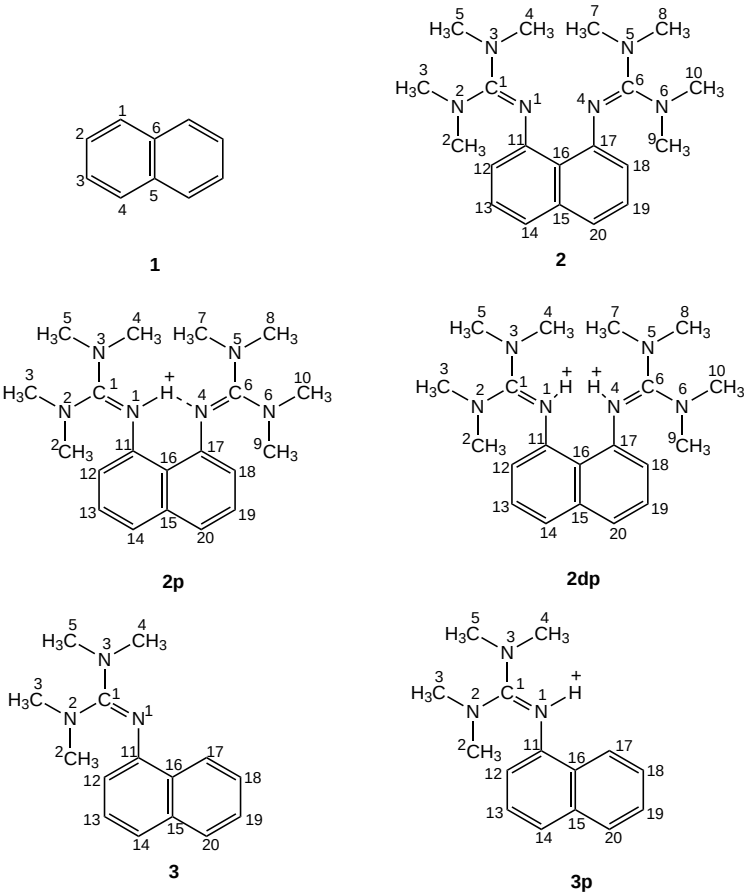

Figure 1. Schematic representation and numbering of atoms in naphthalene **1**, **TMGN 2**, the protonated **2p** and diprotonated **2dp** forms of **TMGN**, and (guanidino)naphthalene, **3**, and its conjugate acid, **3p**.

Table 1. Selected structural parameters of naphthalene **1**, **TMGN** and its protonated and (bis)protonated forms **2p** and **2dp**, respectively, as calculated by the HF/6-31G* model (distances in Å and angles in degree).[a]

Bond/Angle	**1**	**2**	**2p**	**2dp**(*anti*)[b]
C(11)–C(12)	1.358	1.370	1.360	1.362
	[1.371][a]	[1.382]	[1.367(7)]	[1.385(10)]
C(12)–C(13)	1.416	1.407	1.411	1.409
	[1.412]	[1.399]	[1.405(7)]	[1.395(12)]
C(13)–C(14)	1.358	1.354	1.354	1.354
	[1.371]	[1.353]	[1.352(8)]	[1.339(12)]
C(14)–C(15)	1.420	1.419	1.422	1.420
	[1.422]	[1.417]	[1.426(7)]	[1.437(10)]
C(15)–C(16)	1.409	1.418	1.416	1.418
	[1.420]	[1.423]	[1.432(6)]	[1.413(10)]
C(11)–C(16)	1.420	1.441	1.435	1.435
	[1.422]	[1.435]	[1.445(7)]	[1.439(10)]
C(11)–N(1)	–	1.398	1.423	1.442
	[1.401(3)]	[1.409(6)]	[1.428(9)]	
C(1)–N(1)	–	1.264	1.330	1.354
	[1.281(3)]	[1.351(6)]	[1.344(10)]	
N(4)–C(6)	–	1.264	1.293	1.354
	[1.283(3)]	[1.326(6)]	[1.369(10)]	
C(1)–N(2)	–	1.388	1.334	1.325
	[1.384(1)]	[1.342(7)]	[1.354(12)]	
C(1)–N(3)	–	1.386	1.336	1.329
	[1.383(1)]	[1.310(7)]	[1.325(11)]	
bond/angle	**1**	**2**	**2p**	**2dp**(*anti*)[b]
N(1)–H	–	–	1.008	0.996
		[0.91(6)]		
N(1)···N(4)	–	2.790	2.683	2.838
	[2.717(3)]	[2.593(5)]		
C(11)···C(17)	–	2.548	2.550	2.567
	[2.519(3)]	[2.553(7)]		
C(11)–C(16)–C(17)	–	124.3	124.9	126.9
	[122.6(2)]	[124.6(4)]		
N(1)–C(11)–C(16)–C(15)	–	−170.4	–8.5	173.5
	[−161.6(2)]	[−2.6(7)]		
C(1)–N(1)–C(11)–C(12)	–	63.0	39.3	41.3
	[57.7(3)]	[−10.3(8)]		

[a] Experimental data, given within brackets, are taken from ref. [25]. [b] Both protons are in more stable *anti*-conformation.

The data reveals that **TMGN** has C_2 symmetry and that 1,8-disubstitution by the tetramethylguanidine group exerts a relatively weak influence on the naphthalene framework in **2**. For instance, bonds which are involved in these substitutions, C(11)–C(12) and C(11)–C(16), are elongated by ≈0.01 Å, and similarly the C(11)–C(16) and C(16)–C(16) bond lengths increase by 0.02 Å. This represents the tendency of the naphthalene skeleton to minimize repulsion between guanidine fragments. The remaining C–C bond lengths are slightly compressed with the exception of *d*[C(15)–C(16)]. Concomitantly, the distance between carbon atoms, C(11)···C(17), increases by 0.062 Å and between C(14)···C(20) decreases by 0.039 Å in relation to the parent compound **1**. The unshared electron pairs assume a roughly antiparallel conformation to minimize their replusion. As a consequence, the imine nitrogens are not in the plane of the molecule and the guanidine groups exhibit an out of plane bending, which is reflected in the N(1)–C(11)–C(16)–C(15) dihedral angle of 10°.

The side view of **2** is given in Figure 2. The guanidine subunits, which are defined by, for example, C(1)=N(1), C(1)–N(2) and C(1)–N(3) bonds, are perfectly planar and in agreement with X-ray measurements, apart from the methyl groups.[25] In contrast, the amine nitrogens are pyramidalized. A useful index of pyramidalization is provided by DP(%), which stands for a degree of pyramidalization.[28] It is calculated by the summation of bond angles α_i ($i = 1-3$) in degrees of the apical nitrogen in question:

$$\mathrm{DP}(\%) = \left[360 - \sum_{i=1}^{3} \alpha_i\right] \Big/ 0.9\,(\%) \quad (4)$$

The DP(%) values of nitrogens N(2) and N(3) are 4.5 and 10.4%, respectively. The naphthalene frame is only slightly nonplanar as evidenced by negligible degrees of pyramidalization of the ring carbons C(11), C(12) and C(16) which assume values 0.5, 0.1 and 0.0%, respectively. It follows, therefore, that the aromatic system retains its aromaticity. It is interesting that the C(11)–N(1) bond length is very similar to that of **DMAN**,[29] despite the fact that imine nitrogen has higher s-character in this bond in the latter compound. Consequently, we can conclude that there is no conjugation between the ring and substituted fragments. This is corroborated by a large dihedral angle C(1)–N(1)–C(11)–C(12) ≈60°, which places the first guanidine group above and the second below the molecular plane. On the other hand, C(1)–N(2) and C(1)–N(3) bond lengths are close to those in free guanidine. This implies that there is an appreciable π-backbonding (n–π* resonance) effect present within the same fragment, which approximately assumes 28 kcal mol^{-1}, as we have shown earlier.[23]

These findings are in accordance with X-ray results.[25] Discrepancies that are found in C(1)=N(1) bond length and the nonbonded N(1)···N(4) contact length are as expected, since it is known that the HF model underestimates the double bond lengths and overestimates nonbonded distances. The structural characteristics of **2** indicate that the system minimizes the intramolecular nonbonded interactions occuring from steric crowding. In order to support and illustrate this conjecture we made use of the concept of homodesmotic reactions:[30]

$$\mathbf{2} + \mathbf{1} \rightarrow 2 \times \mathbf{3} + \boldsymbol{\varepsilon}_1 \quad (5)$$

The MP2 model yields 0.7 kcal mol^{-1} for ε_1; this provides convincing evidence that there is neither an unfavourable

  0947-6539/02/0807-1696 $ 20.00+.50/0 *Chem. Eur. J.* **2002**, *8*, No. 7

steric congestion repulsion nor a significant angular strain effect in the naphthalene ring deformation. It follows that the high proton affinity of this compound (see below) does not have its origin in the repulsion of nitrogen lone pairs in the initial base.

TMGN is a polyfunctional base and an interesting question is which site is the most basic. Our previous experience with guanidines and polyguanides[23] suggests that the imine nitrogen is preferred for two reasons: 1) it induces a very strong cationic resonance and 2) it allows for the formation of a relatively strong intramolecular hydrogen bond (IHB). This is indeed the case, as both experiment[25] and the present calculations show. The strength of the IHB can be conveniently estimated by Equation (6):

$$\mathbf{2p} + \mathbf{1} \rightarrow \mathbf{3} + \mathbf{3p} + \varepsilon_1^+ \qquad (6)$$

Equation (6) yields $\varepsilon_1^+ = -11.8$ kcal mol^{-1}. Hence, the intramolecular hydrogen bonding contributes considerably to the basicity of **TMGN**.

Proton attack causes substantial changes in the geometry of **2p**. The naphthalene frame becomes completely planar. The amino groups undergo significant planarization too, as shown by their low degrees of pyramidalization (DP(N2) = 0.2% and DP(N3) = 0.9%). This is a consequence of a strong cationic resonance effect within the same guanidine moiety. Concomitantly, the C(1)–N(1) bond length increases by 0.066 Å, whereas C(1)–N(2) and C(1)–N(3) bond lengths decrease by 0.05 Å. Interestingly, the other guanidine subunit also exhibits noticeable planarization. For instance, pyramidalization indices drop to DP(N5) = 2.8% and DP(N6) = 1.3%, which implies a decrease of 1.7% and 9.1%, respectively, relative to the neutral base **2**. This is accompanied by changes in interatomic bond lengths of N(4)=C(6), C(6)–N(6) and C(6)–N(5) by 0.029 Å, −0.021 Å and −0.025 Å, respectively. It also follows that protonation at N(1) triggers cationic resonance within the N(4) guanidine fragment. We are tempted to conclude that the second guanidine fragment is also *partially* protonated. The changes in bond lengths approach roughly 50% of the magnitude of changes found in the directly-protonated guanidine fragment. It should be mentioned that other authors have considered the hydrogen bonds either as the first stage of protonation or as the incipient state of a proton transfer process that leads to formation of the zwitterionic ion pairs.[31] However, our finding that intramolecular hydrogen bonding can trigger an appreciable resonance effect in the neighbouring guanidine fragment in the protonated species is new, and illustrates how the introduced positive charge of the proton causes substantial polarization and redistribution of the electron density, which has important chemical consequences. There is no doubt that the resonance effect triggered by partial protonation stabilizes the conjugate acid **2p** or, in other words, amplifies the basicity of **2**. Finally, it is worth noting that C(11)–N(1) bond length increases by 0.025 Å through rehybridization of N(1) atom on protonation.

Protonation decreases the dihedral angle C(1)–N(1)–C(11)–C(12) between the naphthalene ring and the directly-protonated guanidine fragment by some 20°. The hydrogen bridge N(1)–H$^+$ ··· N(4) leads to a decrease in the nonbonded contact N(1) ··· N(4) by 0.1 Å, which compares well with the experimental estimate of 0.12 ± 0.05 Å.[25] The hydrogen bond is asymmetric and nonlinear. The N(1)–H$^+$ bond length and the N(4) ··· H$^+$ contact length which are related to a partial protonation assume 1.008 and 1.882 Å, respectively. The bridging angle N(1)–H ··· N(4) angle is 134.1° which represents a deviation from linearity by 46°. The general agreement with measured structural data (Table 1) is good, despite that the experimental parameters were gathered from a crystal salt of **TMGN** with PF_6. Consequently, the experimental results involve influence of intracrystal forces and the thermal smearing effect. The former includes rather strong Coulombic interaction between **TMGN** and the counterion. Theoretical results refer to a frozen free molecule.

Diprotonation poses another interesting problem in relation to the attachment of a second proton. One expects that the second proton would be placed at one of four amine nitrogens on the periphery of the molecular system in order to diminish the interproton repulsion. However, both theoretical calculations and subsequent X-ray analysis[25] have shown that the second proton attack occurs at the free imine nitrogen, and this underlines the importance of the resonance effect within the guanidine moiety. The crystal structure parameters for **2dp** were collected for two different complexes: a) the first was obtained through a solution with CH_2Cl_2 leading to a [**2dp**][Cl,Cl_2H] adduct and b) the second was prepared employing a treatment with HPF_6 (involving HBF_4 as an impurity) resulting in [**2dp**][PF_6,BF_4] complex. The former complex has two protons in a *syn*-conformation that take part in hydrogen bonding to a chloride anion bridge, whereas the latter has two protons in a *anti*-conformation. It was concluded that *syn*- and *anti*-conformation cannot differ greatly energetically.[25] Our calculations indicate that, as expected, the *anti*-conformation is more stable by 3.5 kcal mol^{-1}. We note that in the *syn*-conformation **2dp**(*syn*) of a free species the protons try to avoid each other, as shown in Figure 2, in contrast to the experimental situation, in which they are stabilized by the counterion.

Repulsive interactions in either **2dp**(*syn*) or **2dp**(*anti*) are not easily estimated. Consider for example the homodesmotic reaction in Equation (7).

$$\mathbf{2dp}(anti) + \mathbf{1} \rightarrow 2 \times \mathbf{3p} + \varepsilon_1^{++}(anti) \qquad (7)$$

MP2 calculations show that $\varepsilon_1^{++}(anti)$ is very high with a value of 54.3 kcal mol^{-1}. $\varepsilon_1^{++}(syn)$ is higher than that by 3.5 kcal mol^{-1}. These values cannot be simply ascribed to nonbonded repulsions in **TMGN**(*anti*) and **TMGN**(*syn*), respectively. Rather, they reflect the difference between the consecutive diprotonation of **TMGN** and two single protonations of **3**. This difference has several contributions. Firstly, the secondary protonation eliminates the intramolecular hydrogen bonding, which occurs in **2p**. Secondly, the primary protonation profoundly changes the electron distribution and orbital energies in **TMGN**, which has some far-reaching consequences. For example, molecular orbitals in **2p** are substantially stabilized and this includes the orbital that describes the lone pair of the imine N(4) atom. Therefore, a

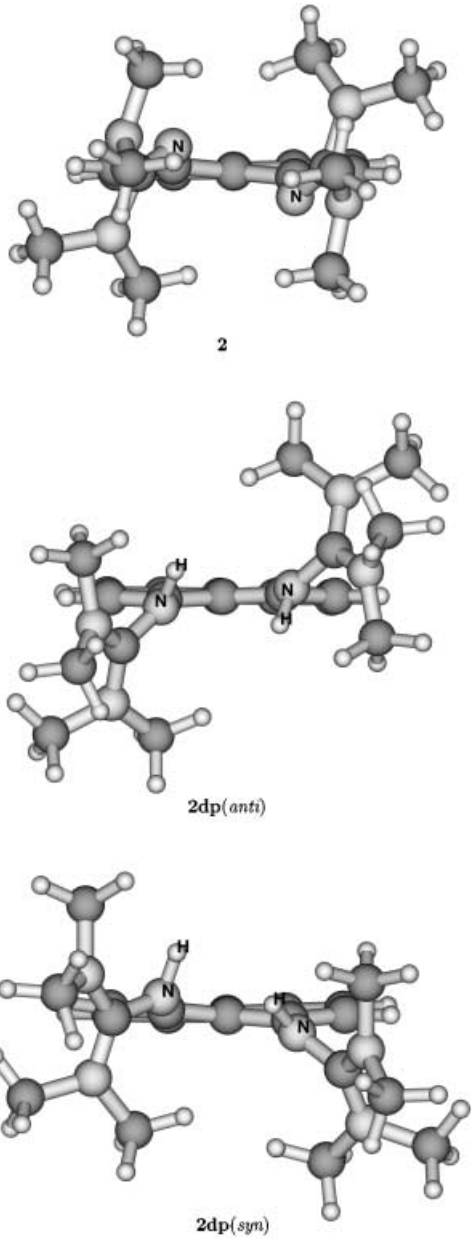

Figure 2. Side view along the C_2 symmetry axis of **2**, **2dp**(*anti*) and **2dp**(*syn*).

higher cost is paid in energetic terms, when the new N(4)–H^+ bond is formed. On top of that, there is a nonbonded repulsion between the two protonated guanidine groups, which is very difficult to delineate.

We give now a brief account of the structural features of the more stable conformation **2dp**(*anti*). The nonbonded contact lengths, C(11)···C(17) and N(1)···N(4), assume large values of 2.567 Å and 2.838 Å, respectively, and the C(11)–C(16)–C(17) angle increases to 127° which indicates angular strain in the naphthalene frame. These theoretical results are in good agreement with the X-ray data for the crystal complex [**2dp**][PF_6,BF_4] (Table 1) and reflect increased repulsion between the protonated guanidine moieties. The naphthalene backbone is planar and its bond lengths do not reveal any significant conjugation with guanidine fragments despite the reduction of the dihedral angle C(1)–N(1)–C(11)–C(12) to 41.3°. This is in line with our earlier finding that protonation triggers the cationic resonance over the C=N bond, which behaves in this sense as the resonance "conductor".[23] In contrast, the single C–N bond of the protonated center (imine nitrogen) acts as an "insulator" for the resonance transmission. It is interesting to observe that C(1)–N(1) bond length increases along the series **2**, **2p** and **2dp** with values of 1.204, 1.330 and 1.354 Å, respectively, which indicates amplification of the resonance effect along this series. The rather long C(1)–N(1) bond in **2dp** is due to the lack of hydrogen bonding between the N(1)···N(4) nitrogens (each guanidine is fully protonated by its own proton). In other words, the proton attached to one imine nitrogen is not shared with the lone pair of the neighbouring imine counterpart and does not participate in its partial protonation. This is also reflected in N(1)–H bond length, which is 0.012 Å shorter in **2dp**(*anti*) than in **2p**. The latter finding is unsurprisingly not reproduced by experiment, as X-ray crystallography does not give precise positions of hydrogen atoms due to their poor scattering qualities. Moreover, it is found that geometry of hydrogen-bonded bridges changes significantly in going from the room to low temperatures.[32, 33] Again, the experimental structure refers to a complex with a counter-ion rather than to a free compound. It is gratifying that our theorectical methods offer complementary information.

We would now like to place our target molecule **TMGN** in a wider context of the structure and properties of other superbases, which are candidates for efficient "proton sponges". It is of particular interest to explore whether the partial protonation occuring in **TMGN** is an exceptional oddity or a more general phenomenon.

We consider here 4,5-bis(tetramethyl-guanidino)fluorene (**TMGF**) **5**, shown in Figure 3, as this system may also exhibit the partial protonation pattern. The numbering of atoms is similar to that adopted for **2** for ease of comparison. System **5** is particularly interesting, since it was realized some time ago that fluorene is a better carrier of intrinsically highly basic groups than naphthalene. It has also been argued, for example, that 4,5-bis(dimethylamino)fluorene is a stronger base than **DMAN**, due to the increased hydrogen-bond strength.[34, 36] It is therefore, of two-fold importance to examine the proton affinity of **5** and compare it with that of **TMGN**. In order to get an understanding of the structural properties of **5** and **5p**, one considers first the geometrical characteristics of the parent molecule fluorene **4**. Its relevant structural parameters are presented in Table 2. The fusion of the five-membered ring does not introduce any significant alternation of bond lengths in benzene fragments that flank the central cyclopentadiene ring. This is in agreement with several studies which show that, unlike smaller carbocycles, five-membered rings do not induce significant Mills–Nixon deformations[37] in fused aromatic moieties. However, a five-membered carbocycle exerts some influence on the selectivity in the electrophilic substitution reactions in annelated systems.[38] Interestingly, disubstitution of guanidine groups in **5** does introduce some bond alternation in the benzene fragments. For instance, C(12)–C(13) and C(14)–C(15) bond lengths become slightly shorter. It is worth noting that the

  0947-6539/02/0807-1698 $ 20.00+.50/0 *Chem. Eur. J.* **2002**, *8*, No. 7

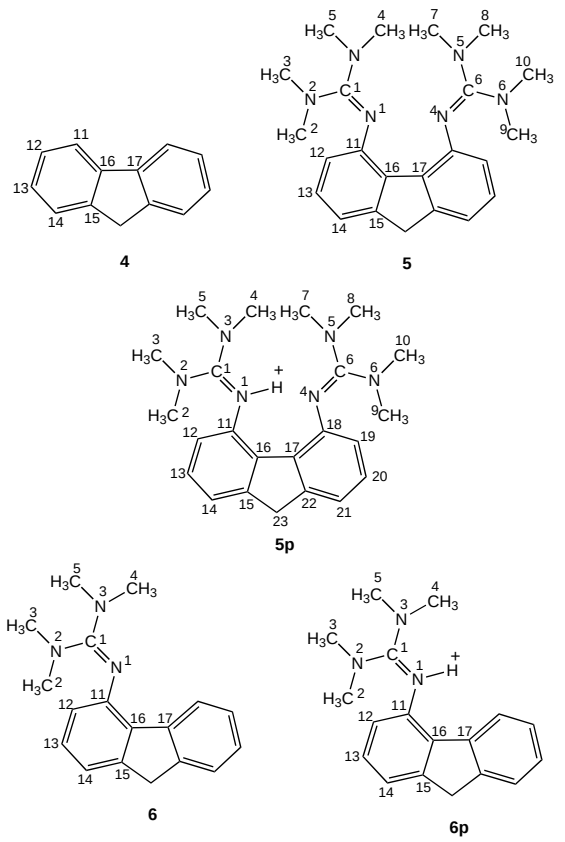

Figure 3. Schematic representation and numbering of atoms in fluorene **4**, TMGF **5**, its conjugate acid **5p**, (guanidino) fluorene **6** and its protonated form **6p**.

Table 2. Relevant structural parameters of fluorene **4**, 1,8-bis(tetramethyl)guanidinofluorene **5**, tetramethylguanidinofluorene **6** and protonated forms **5p** and **6p** as obtained by HF/6-31G* model (distances in Å, angles in degrees.

Bond/Angle	**4**	**5**	**5p**	**6**	**6p**
C(11)–C(12)	1.387	1.401	1.392	1.396	1.388
C(12)–C(13)	1.388	1.379	1.381	1.385	1.383
C(13)–C(14)	1.389	1.384	1.388	1.387	1.389
C(14)–C(15)	1.381	1.377	1.377	1.380	1.387
C(15)–C(16)	1.395	1.404	1.403	1.396	1.400
C(11)–N(16)	1.385	1.403	1.391	1.395	1.386
C(16)–C(17)	1.474	1.502	1.489	1.478	1.479
C(11)–N(1)	–	1.399	1.421	1.397	1.426
C(1)–N(1)	–	1.269	1.332	1.269	1.335
C(1)–N(2)	–	1.376	1.334	1.384	1.330
C(1)–N(3)	–	1.389	1.335	1.384	1.334
N(1)–H	–	–	1.016	–	0.997
N(1)···N(4)	–	3.007	2.804	–	–
C(11)···C(18)	3.291	3.464	3.416	3.313	3.347
C(11)–C(16)–C(17)	131.0	134.3	133.7	130.9	132.5
N(1)–C(11)–C(16)–C(15)	–	170.9	172.3	176.7	176.7
C(1)–N(1)–C(11)–C(12)	–	58.4	41.3	56.1	52.6

bond lengths that belong to the upper part of the perimeter undergo the largest changes (increases) upon disubstitution. Structural parameters that describe the guanidine fragments compare with those found in **2**. The nonbonded contact length N(1)···N(4) is 0.217 Å larger relative to that in **TMGN**. It would be erroneous, however, to conclude that repulsive interactions between guanidine groupings are weaker than in **2**. On the contrary, the corresponding homodesmotic Reaction (8) shows that $\varepsilon_2 = 3.7$ kcal mol^{-1}.

$$\mathbf{5} + \mathbf{4} \rightarrow 2 \times \mathbf{6} + \varepsilon_2 \quad (8)$$

This is surprising at first, as avoidance of the unshared electron pairs of the N(1) and N(4) atoms is more efficient compared with **TMGN** and yet the nonbonded repulsions are higher. Investigation of geometric parameters shows that the CH_3 groups of the two guanidine fragments in **TMGF** are closer together than in **TMGN** which leads to a net repulsion of ≈ 4 kcal mol^{-1}. The preferential proton attack occurs at one of imine nitrogens. The newly formed N(1)–H bond in **5p** has a bond length of 1.016 Å which is 0.008 Å longer than in **2p** (Table 2). The hydrogen bridge is not linear, but bent, and forms an angle (N(1)–H···N(4)) of 151.5° which is closer to planar by 17.4° than the IHB in **2p**. It is useful to get a rough estimate of its strength, which in turn can be operationally identified with a change in the electronic energy of the conceived reaction.

$$\mathbf{5p} + \mathbf{4} \rightarrow \mathbf{6} + \mathbf{6p} + \varepsilon_2^+ \quad (9)$$

$\varepsilon_2^+ = -13.9$ kcal mol^{-1} implies that steric congestion and angular strain in **5** together with the strain relief and hydrogen bonding in **5p** contribute about 17.6 kcal mol^{-1} to the APA of **5**. Strictly speaking ε_2^+ involves some strain energy too, but this does not change our final conclusion. As a consequence, **5** is a stronger base than **2**. A point of interest is a partial protonation of the second guanidine group in **5** starting with N(4) imine nitrogen. It appears that the C(4)=N(6) bond length increases to 1.295 Å, whereas the C(6)–N(5) and C(6)–N(6) bond lengths are compressed to 1.360 and 1.365 Å, respectively, which is analogous to the situation in **2p**. One can conclude that the concept of partial protonation is vindicated and that cationic resonance is operative in the more distant guanidine fragment (relative to the proton), albeit to a lesser extent (roughly 40–50%). It is probably not exaggerated to say that the second guanidine is semiprotonated.

Proton affinities and basicities in acetonitrile: The gas phase proton affinities of molecules **2**–**6** are calculated by the MP2 model and presented in Table 3. They are supplemented by results obtained for systems **7**–**11** (Figure 4), which serve either as reference values or provide useful complementary information for the interpretion the basicity of more complex (super)bases. We begin with a discussion of the fundamental structural and electronic motif of guanidine **8** and consider the increase in its APA as a function of types and number of substituents. Successive methylation leads to enhanced proton affinity, which increases from 233.7 to 249.5 kcal mol^{-1} along the molecules **8**–**10**. High basicity of these simple systems has its roots in pronounced cationic resonance in their conjugate acids, which is an inherent property of the protonated guanidine moiety.[23] This electronic pattern and the accompanying resonance stabilization is complemented by the relaxation effect from CH_3 groups, which leads to even higher basicity. It is remarkable that a simple system such as **10** is

Table 3. Total molecular MP2 energies (in a.u.), zero point vibrational energies and proton affinities (in kcal mol^{-1}) and theoretical pK_a values. Experimental pK_a data are given within square parenthesis.

Molecule	E(MP2)	(ZPVE)$_{sc}$	PA(MP2)$_{gas}$	pK_a(theor)[a]
1	−384.80305	88.3	–	–
TMGN	−1105.67360	290.5	–	–
TMGN(N1)$_p$	−1106.10392	299.3	257.5	25.4[25.1 ± 0.2]
TMGN(N1,N4)$_{dp}$	−1106.40230	307.8	178.7	–
TMGN(N5)$_p$	−1106.36862	307.8	157.6	–
TMGN(N6)$_p$	−1106.36603	307.7	156.1	–
3	−745.24206	189.5	–	–
3p	−745.64622	198.2	244.9	20.5
4	−500.01768	112.6	–	–
5	−1220.89163	314.7	–	–
5p	−1221.32612	323.6	263.7	27.8
6	−860.45700	213.7	–	–
6p	−860.86388	222.4	246.2	20.6
7	−878.83760	233.3	–	–
7p	−879.25598	242.0	253.8	24.6
DMAN	−651.99842	176.1	–	–
DMAN$_p$	−652.40386	185.0	245.5	19.9[18.2][c]
8	−204.87136	46.0	–	–
8p	−205.25450	52.7	233.7	24.1
9	−361.61022	113.5	–	–
9p	−362.02171	121.5	244.6	23.7[23.6]
10	−400.78790	129.7	–	–
10p	−401.19983	138.7	249.5	24.4[25.0]
11	−592.01674	161.3	–	–
11p	−592.42123	170.0	245.1	21.1 [20.6]

[a] Experimental data are taken from ref. [39], if not stated otherwise. [b] Ref. [25]. [c] Ref. [40].

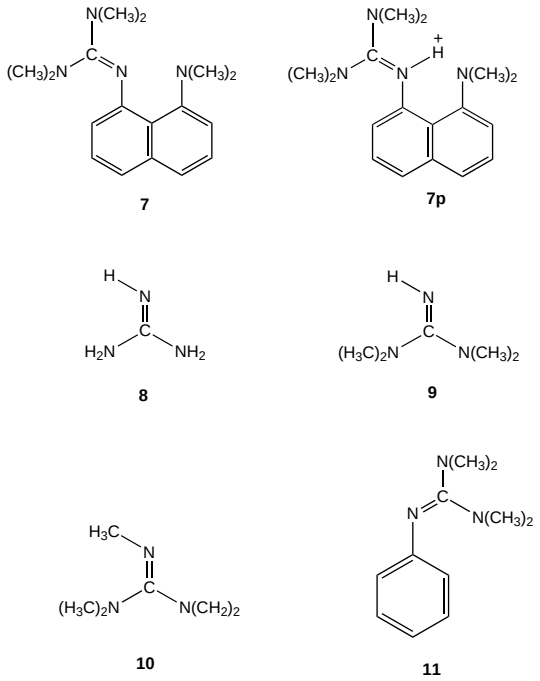

Figure 4. Molecules included in the investigations of the solvent effect in acetonitrile.

more basic than the paradigm, **DMAN**, in the gas phase. This difference is even more pronounced in acetonitrile (see below).

Another point of interest is that tetramethylguanidine, which is attached to a naphthalene fragment that serves as a carrier in **3**, has a proton affinity comparable to that of **DMAN**. An imine–amine combination that possesses lone pairs in a close proximity yields APA of 253.8 kcal mol^{-1} in compound **7**, which increases in our target molecule **TMGN** to 257.5 kcal mol^{-1}. The higher APA in **TMGN** relative to **7** is a result of a weaker IHB in the latter compound as shown by the corresponding homodesmotic reaction, which gave the IHB stabilization of only −5.5 kcal mol^{-1}. However, the most powerful base studied here is **5**, which exhibits an APA as high as 263.7 kcal mol^{-1}. The difference in proton affinities, APA(**5**) − APA(**2**), of 6.2 kcal mol^{-1} can be ascribed in part to the stronger hydrogen bond in **5p** (2 kcal mol^{-1}), and in part to the higher strain in the initial base **5** relative to **2**. Results from Table 3 show that it is 21–22 kcal mol^{-1} more profitable to attach the second proton to the unprotonated imine nitrogen in [**TMGN**]H$^+$(N1) than to protonate either the N(5) or N(6) amino nitrogen atoms.

Recently, we considered basicity of polyguanides and some related neutral (super)bases in acetonitrile.[41] For that purpose we employed the electrostatic model of Miertuš et al.,[42] which was developed within the concept of homogeneous solvent polarized by a solute molecule. In determining the cavities that surround solvated molecules, we followed a suggestion of Wiberg et al.,[43] who used isodensity shells that involve the electronic density of 0.0004 e B^{-3} and gave rise to the isodensity polarized continuum model (IPCM). Since the calculations of pK_a values in acetonitrile ($\varepsilon = 36.64$) require several iterations, we utilize a more economical B3LYP/6-311+G**//HF/6-31G* model, in which ZPVEs are taken from the gas-phase calculations which were evaluated at the HF/6-31G* level. This simple model proved very useful in reproducing the experimental pK_a data for a number of strong neutral nitrogen bases.[41] There was an excellent least square fit correlation between the proton affinities APA(CH_3CN) calculated in acetonitrile and the experimental pK_a values.

$$pK_a(CH_3CN) = 0.4953\,APA(CH_3CN) - 119.7 \quad (10)$$

The high regression coefficient $R = 0.997$ and a low average absolute error (0.4 pK_a) units are evidence of a high correlation of the theoretical results with experimental data. This formula will be used in a predictive manner, but comparison will be made with experimental results whenever possible. The estimated pK_a value for (**TMGN**)H$^+$(N1) of 25.4 is in good agreement with experimental work of Raab et al.,[25] who obtained a pK_a of 25.1 ± 0.2. An interesting discrepancy between theory and experiment is found in **DMAN**, in which the calculated value seems to be too high (Table 3). A part of this disagreement could possibly originate from the fact that the proton in (**DMAN**)H$^+$ is located in a cavity which is formed by four methyl groups and which provides complete protection from solvent molecules.[44] This is not usually the case with compounds used in deriving the empirical Equation (10). Consequently, our estimate of pK_a values for completely or partially protected protons could be too high. Therefore, additional investigations of the basicity of **DMAN** and its derivatives in acetonitrile are highly desirable.

0947-6539/02/0807-1700 $ 20.00+.50/0 *Chem. Eur. J.* **2002**, *8*, No. 7

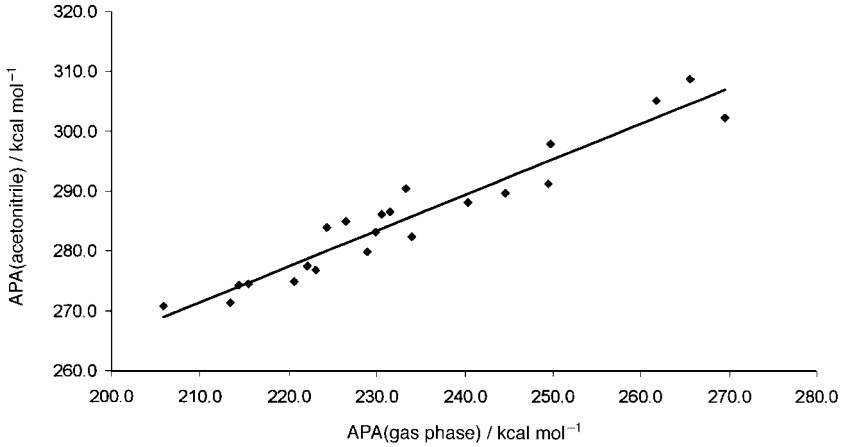

Figure 5. A plot of the absolute proton affinity in acetonitrile against the corresponding gas phase values.

The origin of the basicity in acetonitrile is an interesting question. Our results indicate that the basicity is a result of interplay between two antagonistic effects. The first is given by the intrinsic or gas phase proton affinity, which usually increases with the size of a base. This is a consequence, for example, of a larger number of substituted alkyl groups, which lead to stronger relaxation effects in conjugate acids, or of a larger number of characteristic highly basic fragments like guanidine moieties (as observed in the APA of **TMGN** with respect to **7**). It should be pointed out that the difference in proton affinities, APA(**2**) – APA(**7**), of 3.7 kcal mol^{-1} originates from the stronger IHB, because it is supported by the partial protonation of the second fragment as discussed above. In order to show that the intrinsic gas phase proton affinity determines the proton affinities in acetonitrile to a large extent, we plotted APA(CH_3CN) against APA(gas phase) in Figure 5 for a large number of methyl derivatives of formidine, formamidine and guanidine. Included in this set are cyclopropenimine, *p*-benzoquinonediimine and their amino derivatives as well as vinamidine and the polyguanides published previously.[41] Despite large variation in size and shape of these molecules there is an apparent trend indicating that a larger APA in the gas phase leads to a higher proton afinity in acetonitrile. The relationship, APA(CH_3CN) = 0.5295 · APA (gas phase) + 147.2 kcal mol^{-1}, is not of a good quality, and the regression factor, R^2, is equal to 0.923. There is a large scatter of points which is reflected by the relatively high average absolute error of 2.6 kcal mol^{-1}. This illustrates that the solvent effect must be taken into account for quantitative data and the effect is due to the molecular size effect.[41] The larger conjugate acid systems undergo lower stabilization in polar solvents, since the positive charge spreads over the whole surface of a molecular cation and this implies that its positive charge density on the surface is lower. Consequently, the polarization of the solvent is weaker. This simple physical picture provides a rationale to the fact that APA(**9**) is larger than APA(**8**) by 10.9 kcal mol^{-1} and yet the former compound is slightly less basic in acetonitrile. Similarly, APA(**11**) – APA(**6**) = – 1.1 kcal mol^{-1}, but pK_a(**11**) – pK_a(**6**) = 0.5 is positive which suggests that **11** is more basic when solvated although its intrinsic proton affinity is smaller. The same conclusion holds for the pair of bases, **11** and **3**. However, the intrinsic proton affinity prevails in most cases as shown by results presented in Table 3, and as illustrated, for example, by inequalities pK_a(**5**) > pK_a(**2**) > pK_a(**3**), which hold despite a decrease in size of these molecules.

Conclusion

The spatial and electronic structure of bases **TMGN**, **TMGF** and some related compounds are examined by ab initio computational methods. Particular emphasis is laid upon their gas phase proton affinities and basicities in acetonitrile. The origin of the high proton affinity and the accompanying basicity in acetonitrile was found to arise from the inherent basicity of the guanidine fragment, which is substituted with four CH_3 groups, and from a strong IHB in the corresponding conjugate acid. The strength of the intramolecular hydrogen bond is supported by the partial protonation of the second guanidine moiety, which is not directly attacked by the proton. The latter may be considered to be semiprotonated. Compelling evidence is presented, which shows that the solvent effects are results of two antagonistic factors: 1) gas phase proton affinity and 2) the size of the conjugated acid. In larger cations the positive charge is distributed over the whole molecular surface. At the same time, the positive charge density is lower, which leads to weaker polarization of the solvent.

Acknowledgement

We thank John von Neumann Institut für Computing des Forschungzentrums Jülich, for allocation of the computer time within the project "Computational Design of Strong Organic Superbases". Our thanks also go to Professor J. Sundermeyer for numerous useful discussions.

[1] S. G. Lias, J. F. Liebman, R. D. Levin, *J. Phys. Chem. Ref. Data* **1984**, *13*, 695.
[2] E. P. Hunter, S. G. Lias, *J. Phys. Chem. Ref. Data* **1998**, *27*, 413.
[3] J. Tang, J. Dopke, J. G. Verkade, *J. Am. Chem. Soc.* **1993**, *115*, 5015, and references therein.
[4] H. Oediger, F. Möller, K. Eiter, *Synthesis* **1972**, 591.
[5] a) R. W. Alder, *Chem. Rev.* **1989**, *89*, 1215; b) R. W. Alder, *Tetrahedron* **1990**, *46*, 683; c) A. L. Llamas-Saitz, C. Foces-Foces, J. Elguero, *J. Mol. Struct.* **1994**, *328*, 297; d) H. A. Staab, T. Saupe, *Angew. Chem.* **1988**, *100*, 895; *Angew. Chem. Int. Ed. Engl.* **1988**, *27*, 865; e) E. D. Raczyńska, M. Decouzon, J.-F. Gal, P.-C. Maria, G. Gelbard, J. Vielfaure-Joly, *J. Phys. Org. Chem.* **2001**, *14*, 25.
[6] R. A. L. Peerboom, S. Ingemann, N. M. M. Nibbering, J. F. Liebman, *J. Chem. Soc. Perkin Trans. 2* **1990**, 1825.
[7] E. D. Raczyńska, R. W. Taft, *Bull. Chem. Soc. Jpn.* **1997**, *70*, 1297.
[8] R. Schwesinger, M. Misfeldt, K. Peters, H. G. von Schnering, *Angew. Chem.* **1987**, *99*, 1210; *Angew. Chem. Int. Ed. Engl.* **1987**, *26*, 1165.
[9] R. Schwesinger, H. Schlemper, C. Hasenfratz, J. Willaredt, T. Dimbacher, T. Breuer, C. Ottawa, M. Fletschinger, J. Boele, M. Fritz, D. Putzas, H. W. Rotter, F. G. Bordwell, A. V. Satish, G. Z. Yi, E.-H. Peters, H. G. von Schnering, *Lieb. Ann.* **1996**, 1055.

[10] J. Catalán, J. L. G. de Paz, M. Yáñez, R. M. Claramunt, C. Lopez, J. Elguero, F. Anvia, J. H. Quian, M. Taagapera, R. W. Taft, *J. Am. Chem. Soc.* **1990**, *112*, 1303.
[11] a) J.-L. M. Abboud, T. Cańada, H. Haman, R. Notario, C. Cativiela, M. D. Diaz de Villegas, M. C. Bordejé, O. Mó, M. Yáńez, *J. Am. Chem. Soc*. **1992**, *114*, 4728; b) M. C. Bordejé, O. Mó, M. Yáñez, M. Herreras, J.-L. M. Abboud, *J. Am. Chem. Soc.* **1993**, *115*, 7389; c) G. Bouchoux, D. Drancourt, D. Leblanc, M. Yáñez, O. Mó, *New J. Chem*. **1995**, *19*, 1243.
[12] B. Amekraz, J. Tortajada, J.-P. Morizur, A. I. González, O. Mó, M. Yáñez, I. Leito, D.-C. Maria, J.-F. Gal, *New J. Chem*. **1996**, *20*, 1011.
[13] a) H. Homan, M. Herreros, R. Notario, J.-L. Abboud, M. Esseffar, O. Mó, M. Yáñez, C. Foces-Foces, A. Ramos-Gallardo, M. Martinez-Ripoll, A. Vegas, M. T. Molina, J. Casanovas, P. Jimenez, M. V. Roux, C. Turrión, *J. Org. Chem.* **1997**, *62*, 8503; b) G. Bouchoux, D. Leblanc, O. Mó, M. Yáñez, *J. Org. Chem*. **1997**, *62*, 8439.
[14] A. Bagno, G. Scorrano, *J. Phys. Chem.* **1996**, *100*, 1536.
[15] E. Fujimora, K. Omoto, H. Fujimoto, *J. Org. Chem.* **1997**, *62*, 7234.
[16] A. Szemik-Hojniak, J. M. Zwier, W. J. Buma, R. Bursi, J. H. van der-Waals, *J. Am. Chem. Soc.* **1998**, *120*, 4840.
[17] Z. B. Maksić, M. Eckert-Maksić, in *Theoretical and Computational Chemistry* (Series Eds.: P. Politzer, Z. B. Maksić), *Vol. 5*, *Theoretical Organic Chemistry* (Ed.: C. Parkanyi), Elsevier, Amsterdam, **1998**, p. 203, and references therein.
[18] A. L. Llamas-Saiz, C. Foces-Foces, A. Martinez, J. Elguero, *J. Chem. Soc. Perkin 2* **1995**, 923.
[19] B. Kovačević, Z. B. Maksić, *Chem. Phys. Lett*. **1998**, *288*, 289; B. Kovačević, Z. B. Maksić, P. Rademacher, *Chem. Phys. Lett.* **1998**, *293*, 245.
[20] Z. B. Maksić, B. Kovačević, *J. Phys. Chem. A* **1998**, *102*, 7324.
[21] Z. B. Maksić, B. Kovačević, *J. Phys. Chem. A* **1999**, *103*, 6678.
[22] D. Suárez, J. A. Menéndez, E. Fuente, M. A. Montes-Morán, *Angew. Chem*. **2000**, *112*, 1376; *Angew. Chem. Int. Ed.* **2000**, *39*, 1320.
[23] Z. B. Maksić, B. Kovačević, *J. Org. Chem.* **2000**, *65*, 3303.
[24] B. Kovačević, Z. B. Maksić, R. Vianello, *J. Chem. Soc. Perkin Trans. 2* **2001**, 886.
[25] V. Raab, J. Kipke, R. Gschwind, J. Sundermeyer, *Chem. Eur. J.* **2002**, *8*, 1682–1693, preceding paper.
[26] Gaussian 94 (Revision D.1), M. J. Frisch, G. W. Trucks, H. B. Schlegel, P. M. W. Gill, B. G. Johnson, M. A. Robb, J. R. Cheesman, T. A. Keith, G. A. Peterson, J. A. Montgomery, K. Raghavachari, M. A. Al-Laham, V. G. Zakrzewski, J. V. Otiz, J. B. Foresman, J. Cioslowski, B. B. Stefanov, A. Nanayakkara, M. Challacombe, C. J. Peng, P. J. Ayala, W. Chen, M. W. Wong, J. L. Andres, E. S. Replogle, R. Gomperts, R. L. Martin, D. J. Fox, J. S. Binkley, D. J. Defrees, J. Baker, J. P. Stewart, M. Gordon, C. Gonzales, J. A. Pople, Gaussian, Inc., Pittsburgh, PA, **1995**.
[27] Gamess 1997, M. W. Schmidt, K. K. Baldridge, J. A. Boatz, S. T. Elbert, M. S. Gordon, J. H. Jensen, S. Koseki, N. Matsunaga, K. A. Nguyen, S. J. Su, T. L. Windus, M. Dupuis, J. A. Montgomery, *J. Comput. Chem.* **1993**, *14*, 1347.
[28] Z. B. Maksić, B. Kovačević, *J. Chem. Soc. Perkin Trans. 2* **1999**, 2623.
[29] H. Einspahr, J.-B. Robert, R. E. Marsh, J. D. Roberts, *Acta Crystallogr. Sect. B* **1973**, *29*, 1611.
[30] P. George, M. Trachtman, C. W. Bock, A. M. Brett, *Tetrahedron* **1976**, *32*, 317; P. George, M. Trachtman, C. W. Bock, A. M. Brett, *J. Chem. Soc. Perkin Trans. 2* **1976**, 1222.
[31] L. Gonzáles, O. Mó, M. Yáñez, J. Elguero, *J. Chem. Phys.* **1998**, *109*, 2685; I. Alkorta, I. Rozas, J. Elguero, *Chem. Soc. Rev.* **1998**, *27*, 163; O. Mó, M. Yáñez, L. Gonzáles, J. Elguero, *Chem. Phys. Chem.* **2001**, 465; I. Alkorta, I. Rozas, O. Mó, M. Yáñez, J. Elguero, *J. Phys. Chem. A* **2001**, *105*, 7481.
[32] J. Rozière, C. Belin, M. S. Lehmann, *J. Chem. Soc. Chem. Commun.* **1982**, 388; D. J. Jones, I. Brach, J. Roziére, *J. Chem. Soc. Dalton Trans.* **1984**, 1795.
[33] E. Bartoszak, M. Jaskólski, E. Grech, T. Gustafsson, I. Olovsson, *Acta Crystallogr. Sect. B* **1994**, *50*, 358.
[34] H. A. Staab, T. Saupe, C. Krieger, *Angew. Chem*. **1983**, *95*, 748; *Angew. Chem. Int. Ed. Engl*. **1983**, *22*, 731.
[35] H. A. Staab, M. Höne, C. Krieger, *Tetrahedron Lett.* **1988**, *29*, 1905.
[36] R. Gleiter, W. Schäfer, H. A. Staab, T. Saupe, *J. Org. Chem.* **1984**, *49*, 4463.
[37] For a comprehensive review on the Mills–Nixon effect and its chemical consequences, see: Z. B. Maksić, M. Eckert-Maksić, O. Mó, M. Yáñez in *Pauling's Legacy—Modern Modelling of the Chemical Bond* (Eds.: Z. B. Maksić, W. J. Orwillw-Thomas), Elsevier, Amsterdam, **1999**, p. 47.
[38] M. Eckert-Maksić, Z. Glasovac, N. Novak-Coumbassa, Z. B. Maksić, *J. Chem. Soc. Perkin Trans. 2* **2001**, 1091.
[39] R. Schwesinger, *Nachr. Chem. Tech. Lab*. **1990**, *38*, 1214.
[40] L. A. Kurasov, A. F. Pozharskii, V. V. Kuzmenko, *Zh. Org. Khim.* **1983**, *19*, 859.
[41] B. Kovačević, Z. B. Maksić, *Org. Lett.* **2001**, *3*, 1523.
[42] S. Miertuš, E. Scrocco, J. Tomasi, *J. Chem. Phys.* **1981**, *55*, 117; S. Miertuš, J. Tomasi, *J. Chem. Phys.* **1982**, *65*, 239.
[43] K. B. Wiberg, P. R. Rablen, D. J. Rush, T. A. Keith, *J. Am. Chem. Soc.* **1995**, *117*, 4261; J. B. Foresman, T. A. Keith, K. B. Wiberg, J. Snoonian, M. J. Frisch, *J. Phys. Chem.* **1996**, *100*, 16098.

Received: September 26, 2001 [F3575]

  0947-6539/02/0807-1702 $ 20.00+.50/0